



Study of luminescence, color and paramagnetic centers properties of albite



Nilo F. Cano^{a,b,*}, Lara H.E. dos Santos^a, Jose F.D. Chubaci^a, Shiguelo Watanabe^a

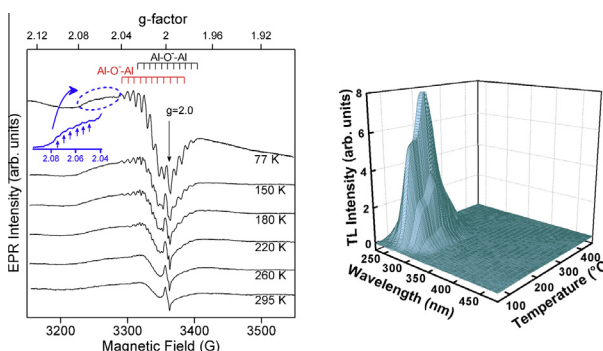
^a Instituto de Física, Universidade de São Paulo, Rua do Matão, Travessa R, 187, CEP 05508-090, São Paulo, SP, Brazil

^b Departamento de Ciências do Mar, Universidade Federal de São Paulo, Av. Alm. Saldanha da Gama, 89, CEP 11030-400, Santos, SP, Brazil

HIGHLIGHTS

- The TL and EPR spectra have been measured in natural albite crystal.
- Albite crystal shows TL peaks at 140, 260 and 350 °C.
- The TL emission spectrum of albite presented bands around 275, 400 and 560 nm.
- The EPR spectrum shows hyperfine lines due to Al–O[−]–Al center superposed on Fe³⁺ signal.

GRAPHICAL ABSTRACT



ARTICLE INFO

Article history:

Received 20 May 2014

Received in revised form 7 August 2014

Accepted 24 August 2014

Available online 3 September 2014

Keywords:

Thermoluminescence

EPR

Optical absorption

Albite

Silicates

ABSTRACT

A sample of natural albite, NaAlSi₃O₈, from the state of Minas Gerais, Brazil, has been investigated. The mineral is a solid solution of K-feldspar (4600 ppm – K) and Ca-feldspar (1100 ppm – Ca). The TL spectra of natural and the pre-annealed at high temperature albite presented a very intense band around 275 nm and weaker bands around 400 and 560 nm. Other TL properties have been investigated through monochromatic (275 nm and 400 nm) glow curves. The EPR spectrum measured at low temperature (77 K) shows the typical 11 lines signal due to Al–O[−]–Al center superposed on Fe³⁺ signal around $g = 2.0$. The EPR spectra above 260 K show only $g = 2.0$ signal due to Fe³⁺ ions.

© 2014 Elsevier B.V. All rights reserved.

Introduction

It is known that the minerals of feldspar group are the most abundant constituents of the Earth's crust. This group is composed of alkali feldspars, plagioclase and celsian subgroup [1].

Albite or sodium feldspar of chemical formula NaAlSi₃O₈ belongs to alkali feldspar subgroup and is one of the end members

of a series of solid solutions with KAlSi₃O₈ as the other end member. Solid solutions of these two feldspars are normally found in nature, but very often 5–10% mixtures of calcium feldspar are also found.

The typical structure of any feldspar mineral contains chains of SiO₄-tetrahedra in two directions perpendicular to their length, formed by the linking of horizontal rings of four tetrahedra.

As in quartz, centers related to O[−], Ti³⁺ and Fe³⁺ are found in feldspars (microclines, orthoclase, plagioclases, etc.). O[−] center develops after irradiation.

* Corresponding author at: Departamento de Ciências do Mar, Universidade Federal de São Paulo, Av. Alm. Saldanha da Gama, 89, CEP 11030-400, Santos, SP, Brazil.

E-mail addresses: nilo.cano@unifesp.br, nfcano@gmail.com (N.F. Cano).

In quartz the aluminum center results from substitution of Si^{4+} in the SiO_4 tetrahedron and after irradiation $[\text{AlO}_4/\text{h}]$ hole center is formed. This center can also be written as shown in Fig. 1(a). Oxygen belonging to two AlO_4 tetrahedron traps hole. Fig. 1(b) is the crystal structure projection in (201)-plane and only aluminum and silicon tetrahedra are shown. Symmetry centers are designated by small crosses. In Fig. 1(c) the most probable assignments of Al–O–Al centers are marked by heavy lines. Fig. 1(a–c) was taken from Petrov [2]. The distinct Al–O–Al centers are designated a_1' , C0, D0, Cm and Dm, each one depending on position of O^- . Thus a_1' , is due to O–Al, C0 to O–C0, D0 to O'–D0, Cm to O'–Cm, Dm to O'–Dm (see Fig. 1(b)).

As feldspar groups of minerals are most abundantly found in the Earth crust and as they are also used in ceramics and glass materials, they form an important class of minerals which can be used in archaeological and geological dating investigations.

In the decades of 1970 and 1980, many investigations on thermoluminescence and radiation effects related to point defects in feldspar have been carried out [3–12]. Defects have been associated with various bands in the optical spectra and the main absorption bands are in the 425–450 nm (blue) and at 700–780 nm (red) region. Telfer and Walker [13] and Marfunin [14] showed that the red band can be attributed to Fe^{3+} ions substituting Al^{3+} in a tetrahedral site. Lehman [10] and Marfunin [14] ascribed the blue band to the Al–O–Al center. Kirsh and Townsend [15] have proposed the following process that takes place for systems with Fe^{3+} ions under irradiation. Electrons and holes created due to irradiation are captured by Fe^{3+} and O^{2-} ions

respectively. When such a mineral is heated, holes are released and recombine with Fe^{2+} ions giving rise to excited Fe^{3+} ions. On transition to the ground state, the excited Fe^{3+} ions emit red light. Furthermore, they suggest a model based on Fe ion to explain the red band (600–800 nm), whereas Speit and Lehmann [7,8] and Marfunin [14] proposed that the Al–O–Al center is responsible for the blue band (400–500 nm).

Santos and Watanabe [16] studied the effects of pre-irradiation annealing at high temperatures on optical absorption, thermoluminescence and electron paramagnetic resonance. They have observed that a pre-irradiation annealing between 800 °C/1 h and 1010 °C/1 h increases the EPR intensity of $g = 2.0$ signal with a maximum around 890 and 920 °C. Heating from 800 to 900 °C increases the magnetic dipole interaction between Fe^{3+} ions while this interaction becomes less effective for heating beyond 920 °C. Further, they have observed that a natural uncolored sample does not change color with 10 kGy irradiation. On the other hand, a 900 °C/1 h pre-heating followed by 10 kGy irradiation produces a strong absorption between 380 and 550 nm and the albite sample becomes colored with orange/red color.

Lowitzer et al. [17] carried out a combined empirical potential and density functional theory calculations of some defects in albite, such as sodium and oxygen vacancies and Schottky defects; supercell, Mott–Littleton approaches coupled to Kohn–Sham density functional method has been used.

The objective of the present work is to study the nature of the luminescence, color and paramagnetic centers in natural albite, measuring the effects of gamma irradiation and thermal treat-

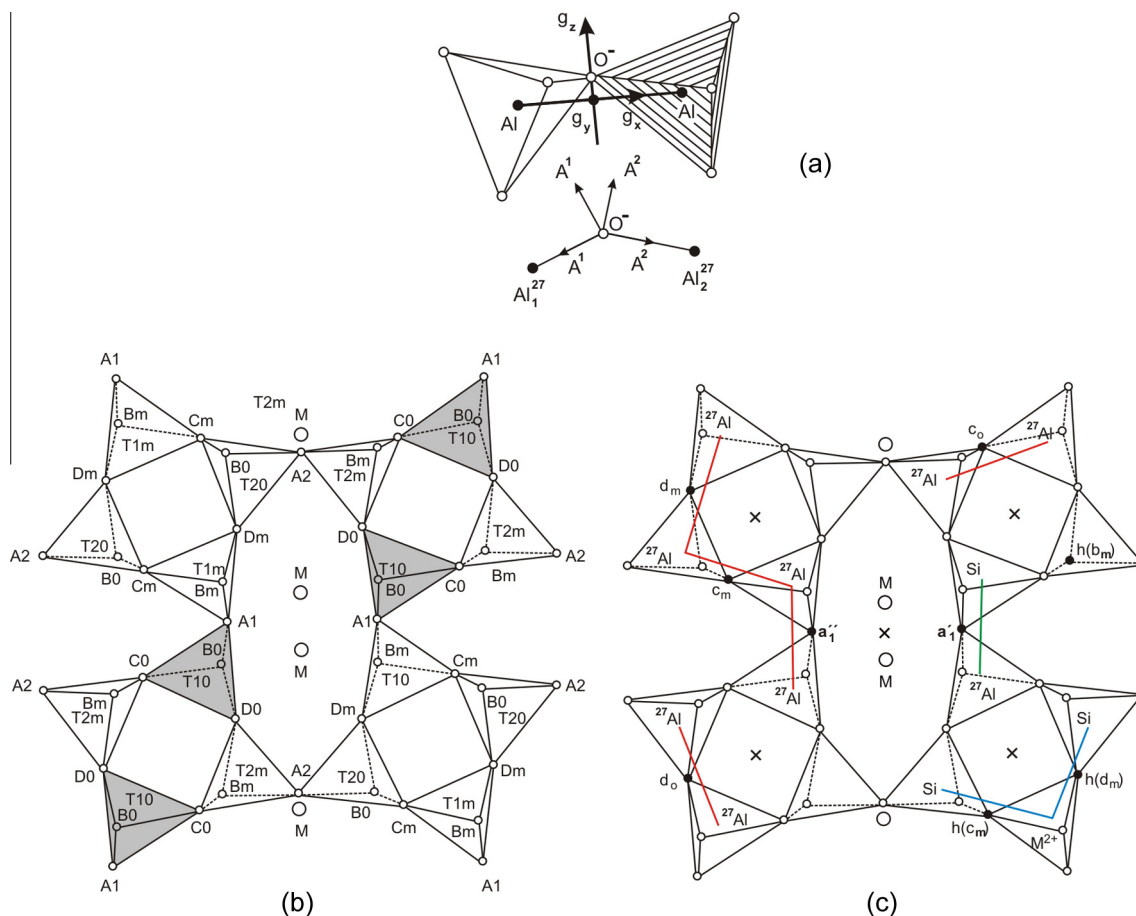


Fig. 1. Position of the Al–O–Al center in feldspar structure. (a) Model of the center: oxygen belonging to two AlO_4 tetrahedron traps hole with formation of O^- . (b) and (c) Projection of the crystal structure feldspar on the (201) plane. In the figure the most probable assignments of different centers Al–O–Al (a_1' , C₀, D₀, C_m, D_m) are marked in red. In blue are marked the most probable sites of centers $\text{SiO}_3^-/\text{M}^{2+}$: h(b_m), (C_m) and h(d_m). In green the center Al–O–/2Na, a_1' . (For interpretation of the references to color in this figure legend, the reader is referred to the web version of this article.)

ments through thermoluminescence (TL), electron paramagnetic resonance (EPR) and optical absorption techniques in an attempt to understand some physical properties and seeking possible applications in the area of ionizing radiation dosimetry of this mineral.

Material and methods

The albite sample investigated here was obtained at the town of Governador Valadares, State of Minas Gerais, Brazil. Its crystal structure was examined by X-rays diffraction (XRD) analysis. The analysis of chemical elements components by X-ray fluorescence (XRF) and XRD measurements have been carried out at the Geology Department of University of São Paulo.

TL measurements of irradiated samples have been carried out on a Daybreak model 1100 reader. For measurements of TL emission spectra and also monochromatic glow curves, a TL reader equipped with UNICROM-100 monochromator and a Hamamatsu 551S PMT was used. A Varian Cary model 550 UV-Vis-NIR spectrometer was used for optical absorption measurements. EPR measurements were carried out on a Bruker X-band EMX spectrometer.

Results and discussion

XRD pattern indicated a similar structure as that of a standard albite system. The analysis of the main components of the albite sample was obtained by XRF. This analysis was performed to identify the chemical elements in the albite sample and for future studies about which of these elements are responsible for the TL and EPR signals. XRF analysis has shown 68.31 wt.% of SiO_2 ,

20.82 wt.% of Al_2O_3 and 11.13 wt.% of Na_2O which are the oxide components of albite and other elements in smaller concentrations. Kirsh and Townsend [15] studied an albite sample with the following main impurities: Ca (0.1 wt.%), Mg (0.1 wt.%), Ti (920 ppm), Fe (600 ppm), Cu (75 ppm) and others in smaller concentration. The albite sample used in the present work has K (1600 ppm), Cu (1100 ppm), Fe (500 ppm), P (400 ppm), Mg (300 ppm), Ti (100 ppm), Cu (25 ppm) and others in smaller concentrations. Therefore the present sample is a solid solution of albite, K-feldspar and anorthite. Furthermore, it is similar to the sample of Kirsh and Townsend concerning main impurities.

Fig. 2 shows the TL emission spectrum of a natural sample and also the emission spectra of sample which was heated to 900 °C/h and subsequently irradiated with 1 kGy gamma irradiation. A strong broad band extending from 240 to 320 nm and a very weak and broad band from 350 to 450 nm are observed. These emissions are due to four TL peaks at 110, 140, 260 and 350 °C. On the other hand, TL glow curves with the emission in the region 270 nm show TL peaks at around 110, 160 and 250 °C. The 250 °C TL peak appears prominent for the emission in the region of 360–420 nm. With 900 °C/1 h pre-irradiation annealing, 120 °C TL peak becomes observable and the 165 °C TL peak moves to 230 °C position.

Kirsh and Townsend [15] have observed both blue and red bands emitted by TL peaks between 100 and 220 °C while Garcia-Grinea et al. [18] suggest that the 275–300 nm, 330–430 nm and 530–580 nm band emissions are due to TL peak around 280–380 °C. In the present work a very intense 240–320 nm band and a weak 350–450 nm band have been observed. We did not look for red band. These emissions are due to 110, 140 and 260 °C peaks and conform more to Kirsh and Townsend [15] results. On the

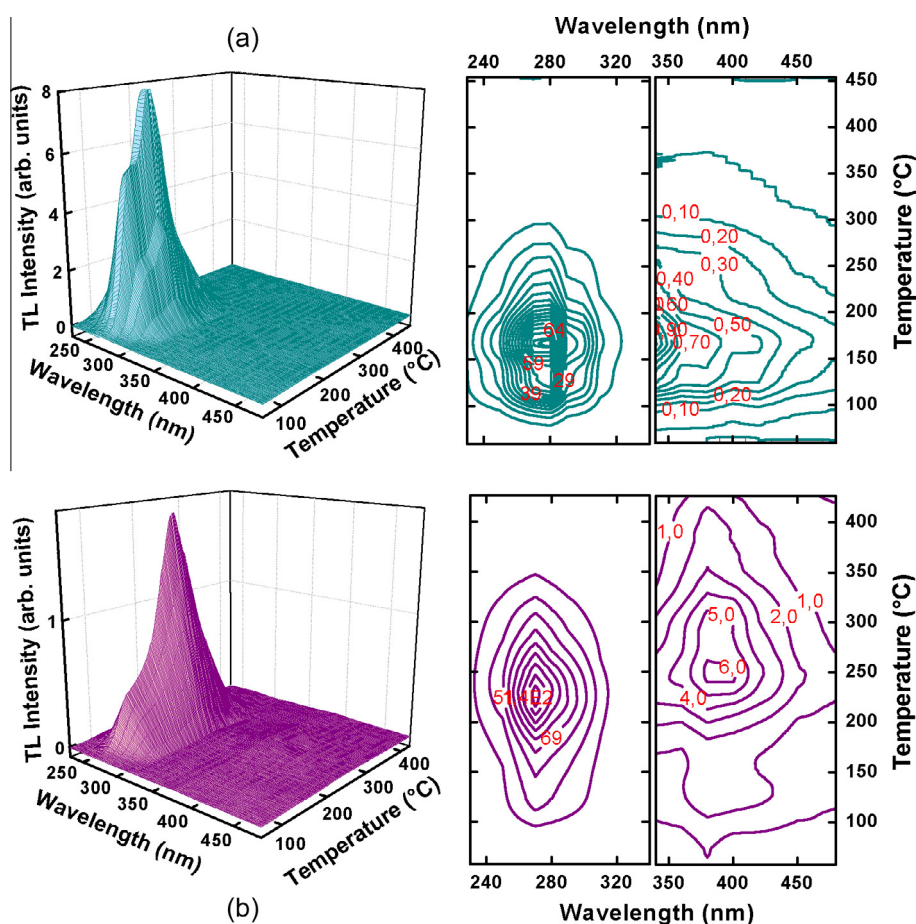


Fig. 2. TL emission spectrum of (a) the sample natural and (b) the sample with pre-heating in 900 °C/1 h and irradiated with a dose of 1 kGy, for wavelengths between 230 and 480 nm.

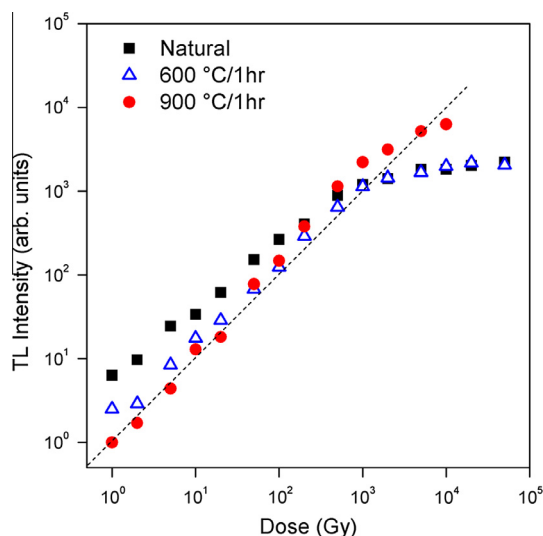


Fig. 3. Behavior of the intensity of monochromatic TL glow curve at 275 nm as a function of radiation dose for natural samples, 600 °C/1 h and 900 °C/1 h annealed and subsequently irradiated with doses between 1 Gy and 100 kGy.

other hand, a 600 °C/1 h annealing followed by 10 kGy gamma-ray irradiation gives a glow curve with 160 (intense), 250 and 350 °C TL peaks. The high temperature pre-irradiation annealing causes displacement of TL peaks to higher temperature.

The intensities of main peak of natural, 600 and 900 °C/1 h annealed samples submitted to gamma-irradiation with doses ranging from 0 Gy to 100 kGy as a function of radiation dose are shown in Fig. 3. The natural sample carries previous radiation effect and therefore the linear growth is not observed. The 160 °C TL peak in the sample annealed at 600 °C/1 h grows linearly with radiation dose up to about 1000 Gy and saturates beyond this dose. On the other hand, this TL peak grows supralinearly between 10 and 10,000 Gy in a sample annealed at 900 °C/1 h. This indicates that albite can be used as a high dose dosimeter, at least up to 10 kGy.

The results shows that the albite sample with annealing at 900 °C for 1 h and 24 h show that the samples have almost equal TL response under 100–100,000 Gy irradiation indicating no significant changes for annealing from 1 to 24 h.

The peak positions have been observed to shift with radiation dose as well as with pre-irradiation annealing at high temperature. Pre-irradiation annealing at 900 °C or at a higher temperature did not change the 275 nm band while a weak and a very broad band is formed extending from 350 to 550 nm and the originally white colored albite sample now exhibits an orange color.

The 275 nm monochromatic glow curves presented peaks 100 times stronger than corresponding peaks in the 380 nm monochromatic glow curves. The strong TL peak around 160 °C in 275 nm monochromatic glow curve shifts to higher temperatures with pre-irradiation annealing from 600 °C/1 h to 1000 °C/1 h. For 800 °C pre-annealing the peak shifts to 250 °C and for 900 and 1000 °C annealing to 275 °C. For annealing at these last two temperatures, a peak around 300 °C is observed. Such high temperature annealing may introduce some changes in the crystal but such large changes are not expected. A similar behavior is observed for the 250 °C TL peak in the 380 nm monochromatic glow curve.

Fig. 4 shows the effects of fluorescent lamp light irradiation at room temperature. For the emission at 270 nm, practically no TL peaks are observed after four days of irradiation while TL peaks with 30–40% intensity remains corresponding to the emission at 380 nm.

Fig. 5 presents EPR spectra taken in the region from 77 to 295 K; it shows clearly the $g = 2.0$ signal due to Fe^{3+} ion, which is not affected by the temperature. The hyperfine lines, however, are

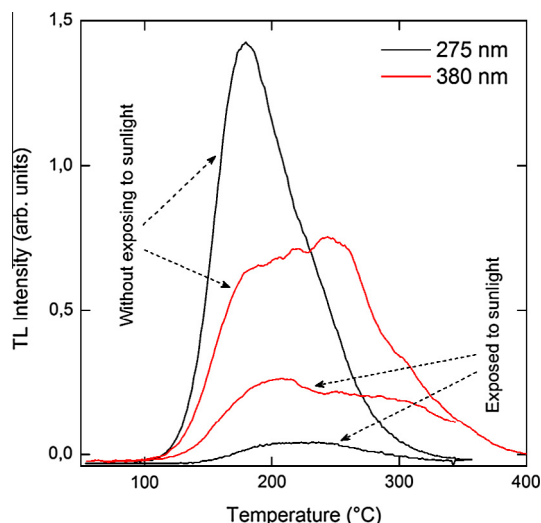


Fig. 4. TL glow curves of samples after exposure to room fluorescent lamp light.

temperature dependent. They are not visible above 260 K. An EPR signal in approximately 1500 G is observed when the spectrum extends from 1000 to 6000 Gauss, this signal is due to the Fe^{3+} ion with a g -value of 4.3. The EPR spectrum also shows additional 6 lines in the region between $g = 2.08$ and 2.04, these lines can be due to Fe^{3+} with spin 5/2, since our sample did not show Mn as impurity. This result is shown in the inset of Fig. 5 (blue color) with an expanded scale.

The hyperfine signals seen at 77 K gradually become smaller as the temperature increases and above 260 K only the Fe^{3+} signal at $g = 2.0$ is observed.

EPR spectra at low temperature of the albite sample pre-annealed at 600 °C/1 h presents double lines in the region between 3300 and 3400 G. These hyperfine lines observed in the EPR spectrum are due to two distinct Al–O–Al centers characterized by slightly different g -values.

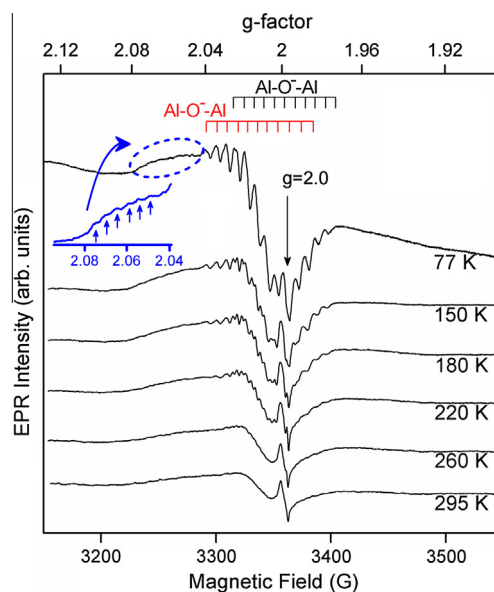


Fig. 5. EPR spectra obtained at different temperatures for the sample pre-annealed in 600 °C/1 h and then irradiated with a gamma dose of 1 kGy. In the inset, EPR spectra in 77 K (blue line) in the region between $g = 2.08$ and $g = 2.04$. (For interpretation of the references to color in this figure legend, the reader is referred to the web version of this article.)

The EPR spectrum of albite at low temperature (77 K) observed in the present study consists of 11 lines and is the same as that found in literature for an Al center. Hyperfine lines arise due to interaction of the unpaired electron with two ^{27}Al nuclei, each one with spin 5/2. This gives 11 lines in the EPR spectrum with intensity ratios of 1; 2; 3; 4; 5; 6; 5; 4; 3; 2; 1 [8,14].

The effects of annealing between 800 and 1010 °C on the EPR spectra of this sample have been reported by Santos and Watanabe [16]. They showed that the samples annealed at 800–1010 °C in steps of 30 °C present EPR signals that grew for temperature around 860 and 900 °C and then decreased. Since this signal is due to Fe^{3+} ions involved in magnetic dipole interactions, the above results in the interval 800–860/890 °C are interpreted as due to the reaction $\text{Fe}^{2+} \rightarrow \text{Fe}^{3+} + e^-$ caused by heating. Above 980 °C, the overgrowth of Fe^{3+} concentration caused some kind of clustering reducing the dipole–dipole interaction. In a smaller scale, a similar behavior has been observed for $g = 4.27 \text{ Fe}^{3+}$ signal.

Kirsh and Townsend [15] have suggested that the concentration of Fe^{3+} ions is reduced due to the reaction $\text{Fe}^{3+} + e^- \rightarrow \text{Fe}^{2+}$ induced by irradiation. In the present work, however, the intensity of $g = 2.0$ signal is observed to grow with dose in contrast to the Kirsh and Townsend [15] model.

The intensity of $g = 2.0$ signal increases significantly with the pre-annealing from 800 °C/1 h to 890–920 °C/1 h and decreasing above these temperatures. It is known that Fe^{3+} has spin $S = 5/2$ and has a magnetic moment such that neighboring iron ions interact through their magnetic dipoles. The annealing at high temperatures such as 800–900 °C enable Fe^{2+} ions to loose one electron giving rise to Fe^{3+} ions and thus increasing the number of Fe^{3+} ions and consequently the dipole (magnetic)–dipole interaction. This explains the increase in the EPR signal ($g = 2.0$) due to 800–900 °C anneal. Anovitz and Blencoe [19] report the melting temperature of albite as being around an average value of $(1100 \pm 20)^\circ\text{C}$. Any annealing above 1000 °C will be close to the melting point of albite so that the crystal structure of albite will be altered resulting in the decrease of EPR signal.

Fig. 6 shows the dependence of EPR intensities of Al–O $^-$ –Al centre and Fe^{3+} ion ($g = 2$) on microwave power. The signal of Fe^{3+} ion saturates around 1–2 mW while the aluminum centre probably saturates beyond 100 mW. Al and Ti centers in SiO_2 are observed to saturate around 100 mW [20]. In the inset of Fig. 6 presents an interesting result where g -values in the range 2.02–1.98 have a dependence on microwave power between 0.010 and 101.0 mW. In this interval of magnetic field we can distinguish a signal with $g = 2$ due to Fe^{3+} ion and a signal at $g = 1.997$ which can be attributed to a Ti-center. In other experiment we carried out an isochronous (15 min) annealing experiments on (natural + 1 kGy) and (900 °C/1 h + 1 kGy) samples, where temperature was varied from 105 up to 300 °C in the first sample and from 105 up to 600 °C in the second sample. In both cases, the EPR signals at $g = 2$ and $g = 1.997$ have been completely annealed away. The same effect was also observed with Al–O $^-$ –Al signals, measured at 77 K.

Fig. 7(a) shows the absorption spectra of natural, 600 °C and 900 °C annealed samples. The inset shows the details in the range 300–800 nm. Fig. 7(b) shows the effect of 10 kGy gamma irradiation on the absorption spectra. A strong UV absorption around 220 nm and a weak absorption band in the visible region are observed. The combined effect of 900 °C annealing and 10 kGy irradiation is to produce an increase in the background absorption by a factor of 1.4 and appearance of a strong and broad band around 410 nm.

The isochronous (15 min) decay experiments show that 220 nm UV band is little affected while the 410 nm band decreases with the temperature, becoming practically zero around 250 °C heating.

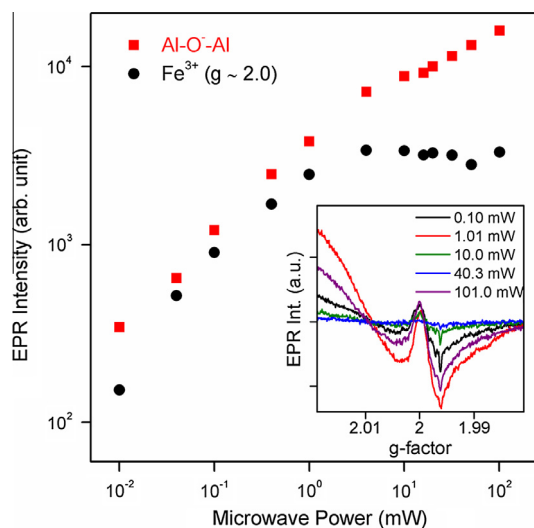


Fig. 6. Intensity as a function of microwave power of the EPR spectrum of the Al–O $^-$ –Al and Fe^{3+} centers at the temperature of 77 K. In inset, the EPR Microwave power dependence between 0.10 and 101 mW for the sample pre-annealed at 600 °C/1 h and irradiated with 1 kGy.

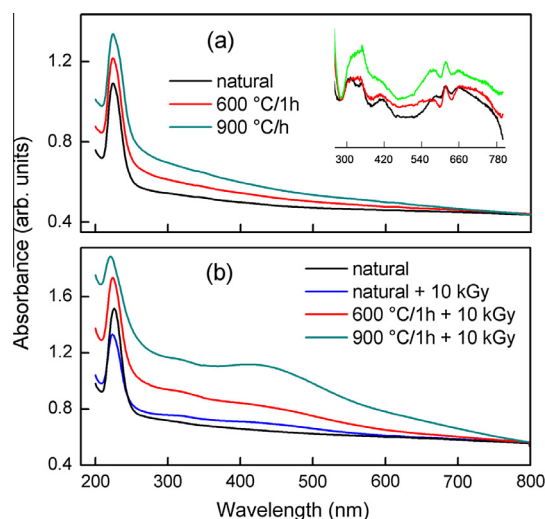


Fig. 7. (a) Absorption spectra of the natural and 600 °C and 900 °C annealed sample in the UV to visible interval and (b) effect of 10 kGy irradiation on samples used in (a).

Fig. 8 depicts the behavior of 220 and 410 nm bands as the temperature is raised from room temperature up to 400 °C. The 220 nm band increases slightly up to 250 °C and then becomes stationary while the 410 nm band starts decreasing around 100 °C and around 220–250 °C decreases to almost zero intensity.

A heat treatment above 900 °C for over 30 min has resulted in the appearance of a broad band extending from 390 to 550 nm and the sample becomes orange colored. This color is observed to disappear after heating this colored sample to 300 °C. Marfunin [14] and several other workers have attributed the red – 780 nm emission to Fe^{3+} ion substituting for Al^{3+} in a tetrahedral site and the blue light emission to Al–O $^-$ –Al. Kirsh and Townsend [15] proposed that electrons liberated during ionization react with Fe^{3+} producing Fe^{2+} ions. During heating for TL read out, the following reaction takes place. $\text{Fe}^{2+} + \text{hole} \rightarrow (\text{Fe}^{3+})^+ \rightarrow \text{Fe}^{3+} + \text{photon}$. The hole can be produced for example, by an O^{2-} ion near Fe^{3+} . On the other hand, in quartz and silicate crystals, oxygen vacancy

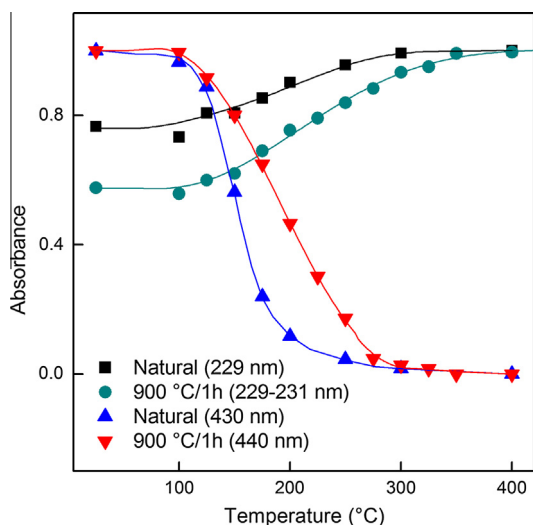


Fig. 8. Behavior of 229–231 nm and 430 nm bands with temperature.

$(V_{\cdot})^{2+}$ is more easily created even at room temperature (see, for instance Rudra and Fowler [21]). During irradiation electrons–holes are produced and two of the electrons can be captured by an oxygen vacancy giving rise to $(V_{\cdot}2e^{-})$ center. As the crystal is heated, according to Toyoda and Ikeya [22], starting around 150 °C one electron is liberated from the above center leaving an oxygen vacancy with one electron, which was denominated as E'_{1} -center. Around 300 °C maximum number of E'_{1} -centers are formed and above this temperature the remaining electron is liberated, such that around 450 °C all the oxygen vacancies are recovered. The electrons liberated in this process are partly captured by a hole center such as $Al-O^{-}-Al$ center emitting 380 nm light or by an aluminum center $[AlO_4/h]$ emitting 470 nm light.

Conclusions

The XRD and XRF analysis have shown that sample studied in the present work is a solid solution of albite, K-feldspar and anorthite.

The TL glow curve of albite shows peaks at 110, 160 and 250 °C. Samples heat-treated at 600 °C for 1 h and irradiated with 10 kGy gamma doses present peaks at 150, 250 and 350 °C. The high temperature pre-irradiation annealing causes displacement of TL peaks to higher temperature.

The TL spectra emission of the albite presents a very intense 260–340 nm band and a weak 350–450 nm band. This result shows that albite has in principle various recombination centers that participate in TL process.

The monochromatic intensity (at 275 nm) of 160 °C TL peak of a sample annealed at 600 °C/1 h grows linearly with radiation dose up to about 1000–2000 kGy and saturates afterwards. In the sample annealed at 900 °C/1 h, this TL peak grows supralinearly

between 10 and 10,000 Gy. As a consequence of the present results, the TL peak at 160 °C (275 nm) may be used for radiation dosimetry.

The EPR spectra of powder sample of albite show eleven hyperfine lines superimposed on the $g = 2.0$ signal. The signal at $g = 2.0$ is attributed to the Fe^{3+} defect in the crystal structure of the albite. The eleven hyperfine lines are due to an $Al-O^{-}-Al$ center. The hyperfine signals due to Al -center seen at 77 K gradually become smaller as the temperature increases and above 260 K only signals at $g = 2.0$ and 4.3 due to Fe^{3+} ion are observed; these signals do not depend upon the temperature.

The EPR spectrum of the albite sample at low temperature presented a spectrum with double hyperfine lines due to two distinct Al centers. Furthermore, additional six lines due to Fe^{3+} ion with spin 5/2 are seen.

The optical absorption spectrum has a very strong band around 275 nm and no absorption bands are observed in the visible region and the crystal is uncolored. The heat treatment in the temperature region 800–1010 °C shows that the Fe^{2+} undergoes the reaction ($Fe^{2+} \rightarrow Fe^{3+} + e^{-}$). It was corroborated by both EPR and optical absorption measurements.

Acknowledgement

The authors wish to thank Ms. E. Somessari and Mr. C. Gaia, Instituto de Pesquisas Energeticas e Nucleares (IPEN), Brazil, for kindly carrying out the irradiation of the samples. This work had financial support from FAPESP and CNPq.

References

- [1] W.A. Deer, R.A. Howie, J. Zussman, *An Introduction to Rock Forming Minerals*, second ed., E. Prentice Hall, 1992, p. 391.
- [2] I. Petrov, *Am. Mineral.* 79 (1994) 221–239.
- [3] D.J. McDougall, *Thermoluminescence of Geological Materials*, Academic Press, London, 1968, pp. 527–544.
- [4] K. Bear, W. Herr, *Earth Planet. Sci. Lett.* 22 (1974) 188–195.
- [5] P.W. Levy, *PACT* 3 (1979) 466–480.
- [6] E.S. Pasternack, A.M. Gaines, P.W. Levy, *Thermoluminescence in ordered and disordered NaAlSi₃O₈*, in: *Proc. Int. Conf. on Defects in Insulating Crystals*, Oak Ridge, Tenn., 1977, pp. 333–334.
- [7] B. Speit, G. Lehmann, *Phys. Status Solidi (a)* 36 (1976) 471–481.
- [8] B. Speit, G. Lehmann, *Phys. Chem. Miner.* 8 (1982) 77–82.
- [9] B. Speit, G. Lehmann, *J. Lumin.* 27 (1982) 127–136.
- [10] G. Lehmann, *NATO ASI Ser.* 137 (1984) 121–162.
- [11] R.A. Akber, J.R. Prescott, *Nucl. Tracks.* 10 (1985) 575–580.
- [12] K. Strickertsson, *Nucl. Tracks.* (1985) 613–617.
- [13] D.J. Telfer, G. Walker, *Nature* 258 (1975) 694–695.
- [14] A.S. Marfunin, *Spectroscopy, Luminescence and Radiation Centres in Minerals*, Springer, Berlin, 1979, p. 135.
- [15] Y. Kirsh, P.D. Townsend, *Nucl. Tracks Radiat. Meas.* 14 (1988) 43–49.
- [16] L.H.E. dos Santos, S. Watanabe, *Radiat. Phys. Def. Solids* 157 (2002) 743–749.
- [17] S. Lowitzer, D.J. Wilson, B. Winkler, *Phys. Chem. Miner.* 35 (2008) 129–138.
- [18] J. Garcia-Guinea, F. Pitalua, V. Correcher, L. Sanchez-Muñoz, F.J. Valle-Fuentes, P. Lopez-Arce, *Bol. Soc. Esp. Ceram.* 43 (2004) 115–118.
- [19] L.M. Anovitz, J.G. Blencoe, *Am. Mineral.* 84 (1999) 1830–1842.
- [20] M. Ikeya, *New Applications of Electron Spin Resonance*, World Scientific Publishing Co., Singapore, 1993, p. 279.
- [21] J.K. Rudra, W.B. Fowler, *Phys. Rev. B* 35 (1987) 8223–8230.
- [22] S. Toyoda, M. Ikeya, *Geochem. J.* 25 (1991) 437–445.